

Supplementary Information

Fluorocarbon Plasma Gas Passivation Enhances Performance of Porous Silicon for Desorption/Ionisation Mass Spectrometry

Rajpreet Singh Minhas^{†,‡,§}, E. Eduardo Antunez^{†,‡}, Taryn M. Guinan^{†,‡,||}, Thomas R. Gengenbach[§], David A. Rudd^{†,‡*} and Nicolas H. Voelcker^{†,‡,§,⊥*}

[†]Drug Delivery, Disposition and Dynamics, Monash University, Parkville, Victoria, 3052, Australia.

[‡]Melbourne Centre for Nanofabrication, Victorian Node of the Australian National Fabrication Facility, Clayton, Victoria, 3168, Australia.

[§]Commonwealth Scientific and Industrial Research Organisation (CSIRO), Clayton, Victoria, 3168, Australia.

^{||}Leica Microsystems, Mount Waverley, Victoria, 3149, Australia.

[⊥]Department of Materials Science and Engineering, Monash University, Clayton, Victoria, 3800, Australia.

*Corresponding author: David A. Rudd, Nicolas H. Voelcker

Current address: Monash Institute of Pharmaceutical Sciences, Monash University, 381 Royal Parade, VIC 3052, Australia.

E-mail: david.rudd@monash.edu, nicolas.voelcker@monash.edu;

Fax: +61 3 9903 9581.

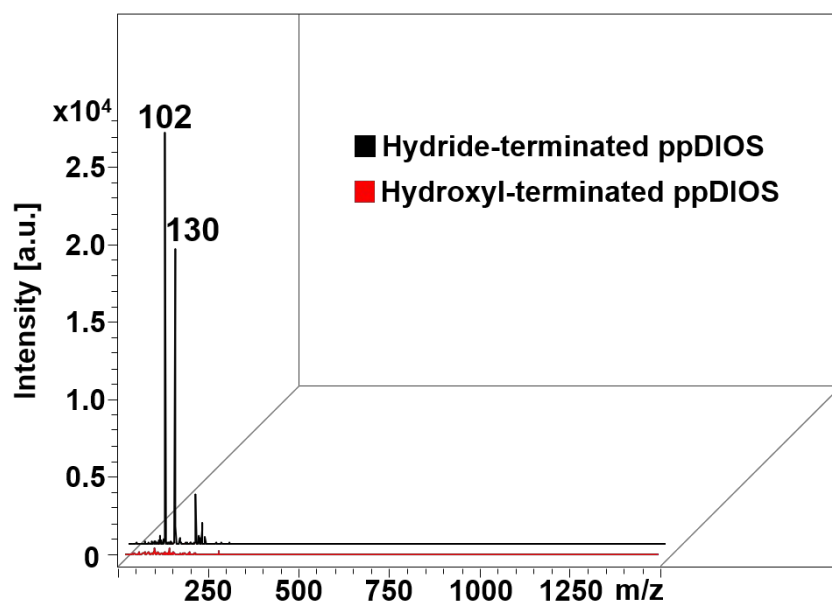


Figure S1: Background mass spectra for freshly etched (hydride-terminated) and ozone-oxidised (hydroxyl-terminated) ppDIOS surfaces. Background peaks are observed at m/z 102, 130, 198 and 212.

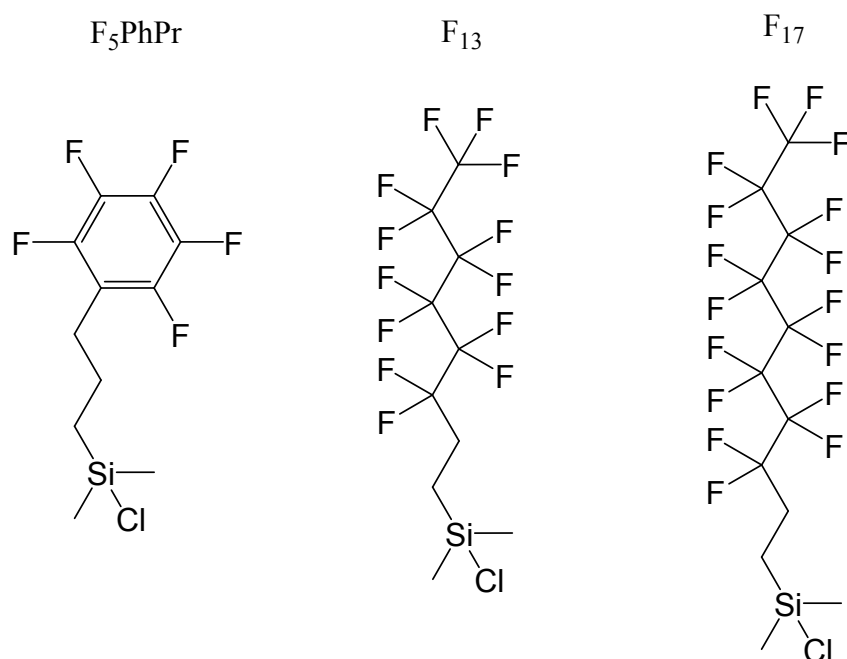


Figure S2. Chemical structures of F_5PhPr , F_{13} and F_{17} , common silanes used to functionalise DIOS surfaces.

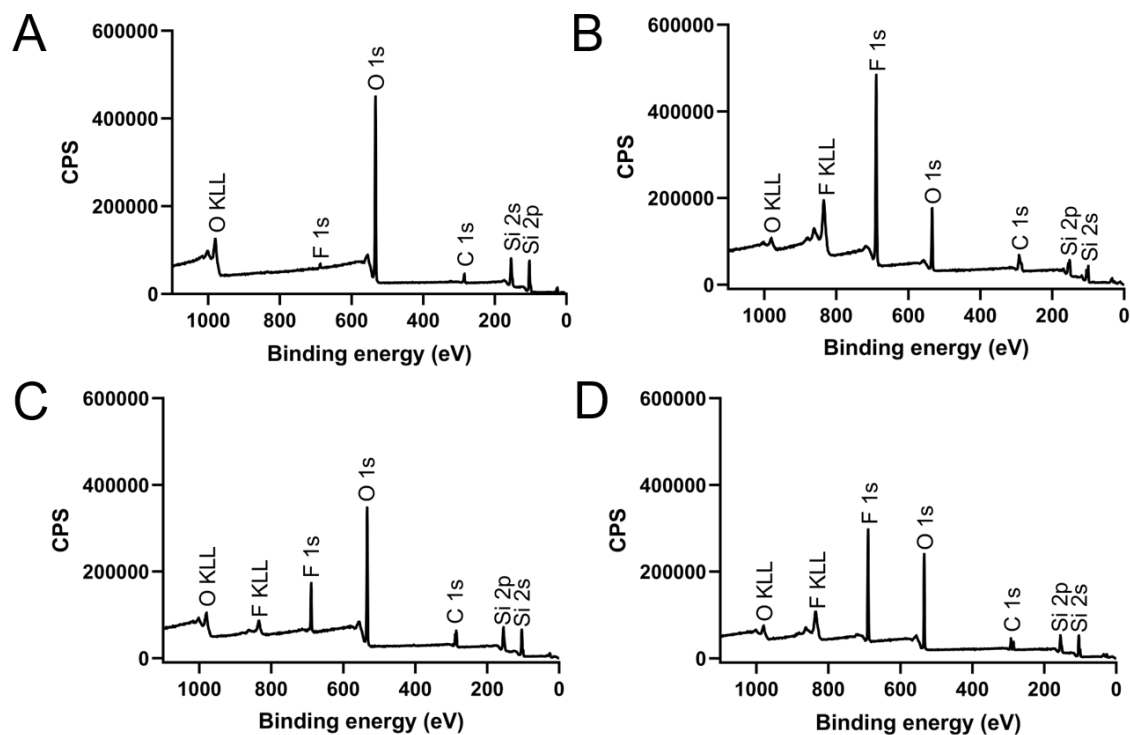


Figure S3: X-ray photoelectron spectroscopy (XPS) survey spectra for DIOS surfaces functionalised via A) ozone-oxidation, B) plasma polymerisation, C) F₅PhPr-silanisation and D) F₁₃-silanisation.

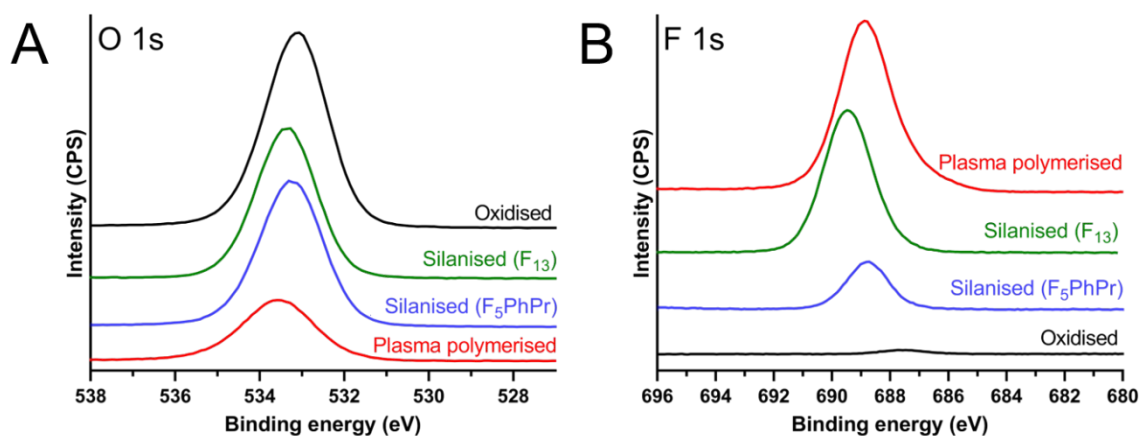


Figure S4: XPS analysis for functionalised DIOS surfaces showing A) high-resolution O 1s spectra and B) high-resolution F 1s spectra.

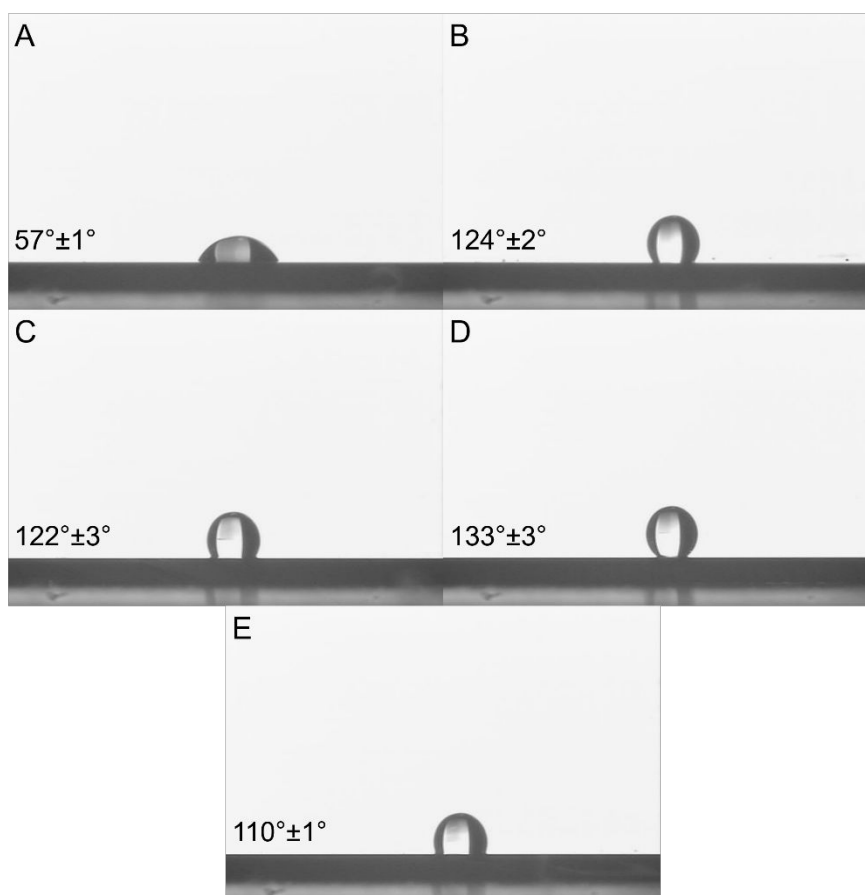


Figure S5: Water contact angle (WCA) measurements for DIOS substrates following A) ozone-oxidation, B) plasma polymerisation, C) F_5PhPr -silane functionalisation, D) F_{13} -silane functionalisation, and E) F_{17} -silane functionalisation. WCA was determined using 1 μ L of water on a contact angle goniometer.

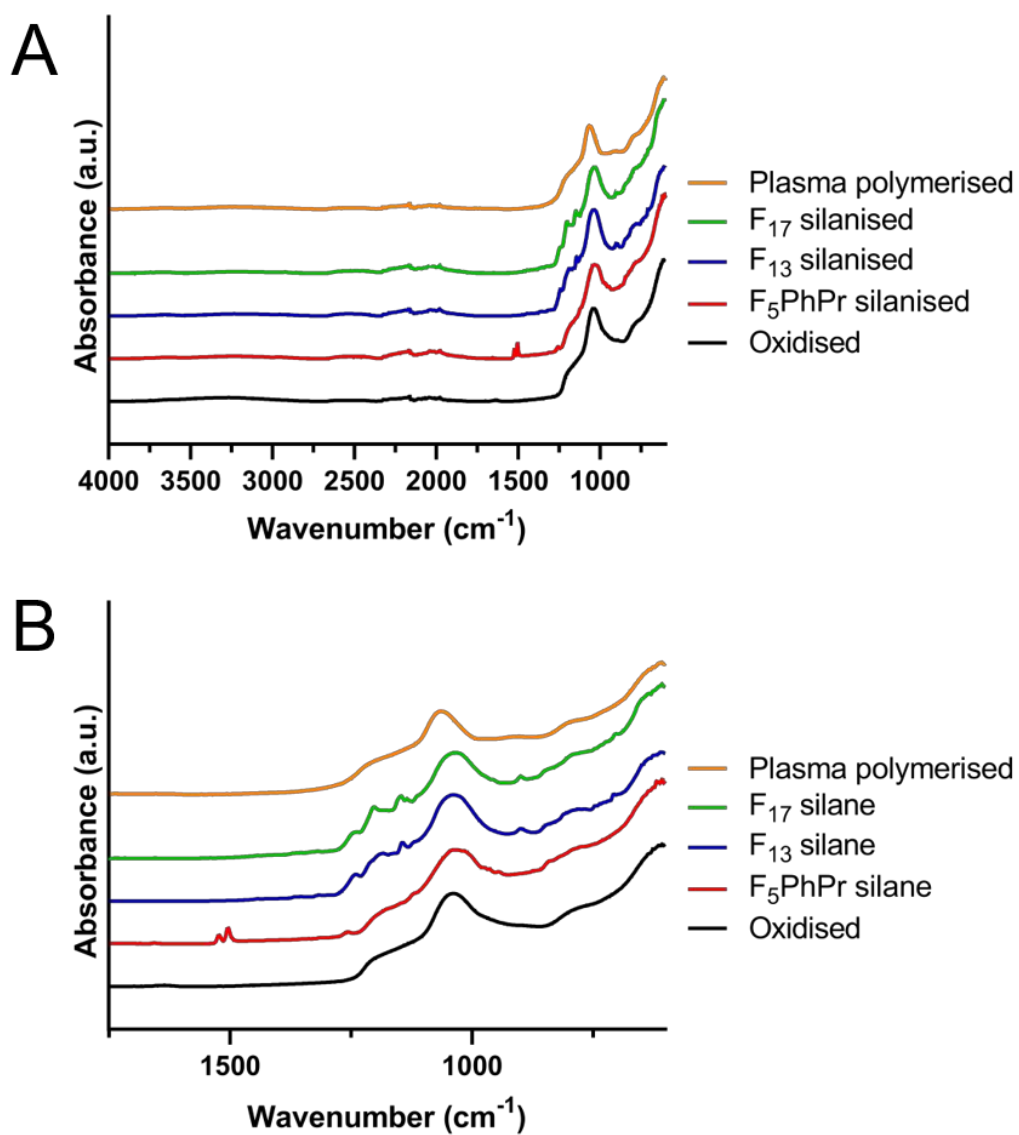


Figure S6. IR spectra overlays of oxidised, plasma polymerised and silanised DIOS surfaces between A) 4000-600 cm^{-1} and B) 1750-600 cm^{-1} .

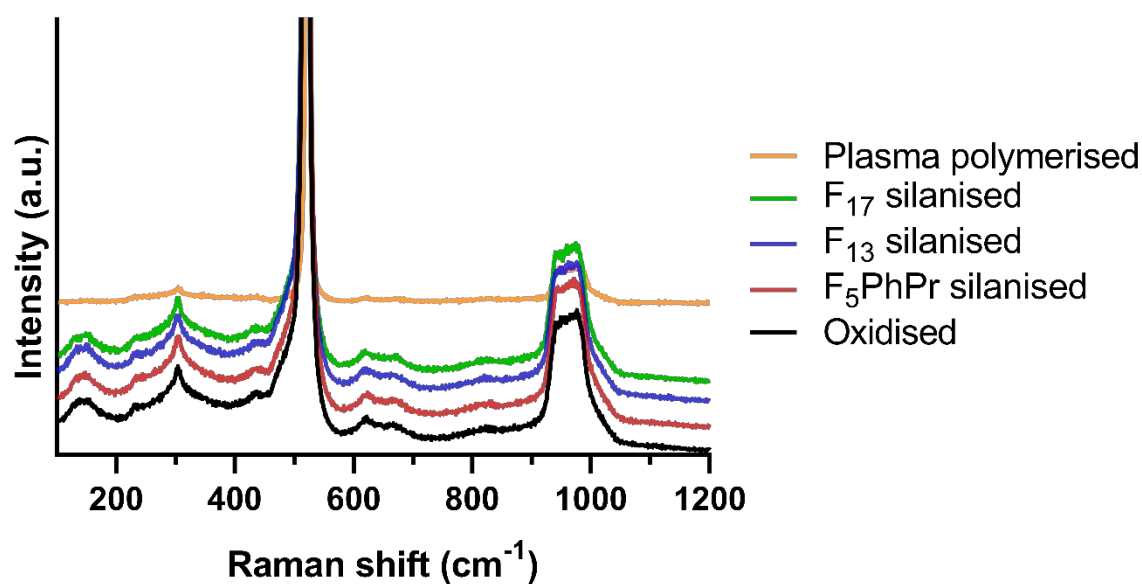


Figure S7. Raman spectra overlays of oxidised, plasma polymerised and silanised DIOS surfaces.

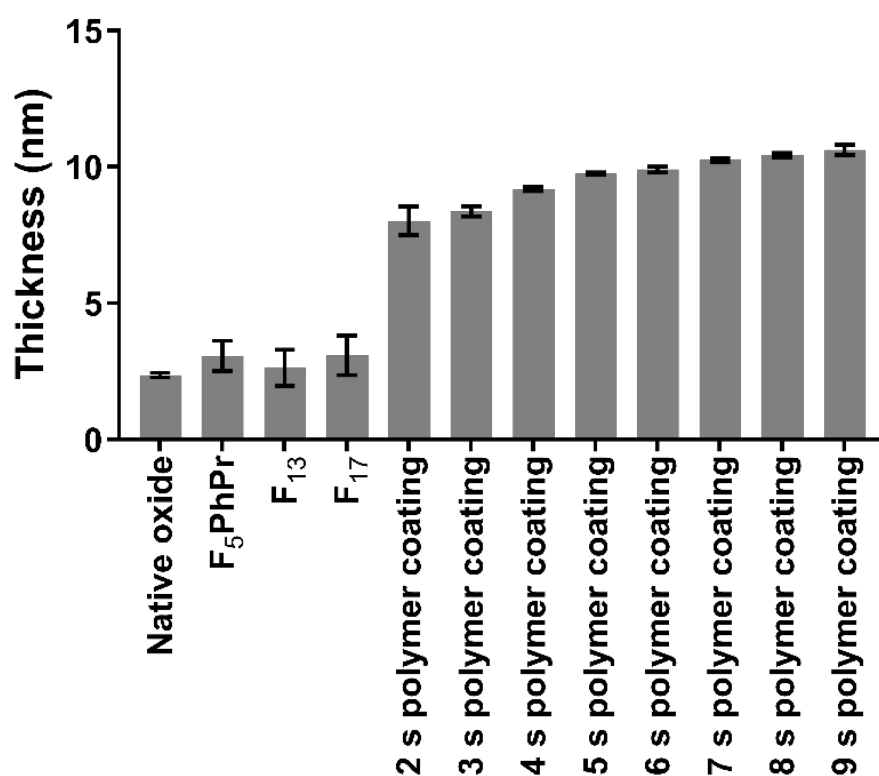


Figure S8: Average thickness of ppDIOS substrates following fluorocarbon gas passivation at various lengths of time. The native oxide layer present on the Si substrate, F_5PhPr , F_{13} and F_{17} -silanes, have been included for comparison. Error bars correspond to the standard deviation (n=3).

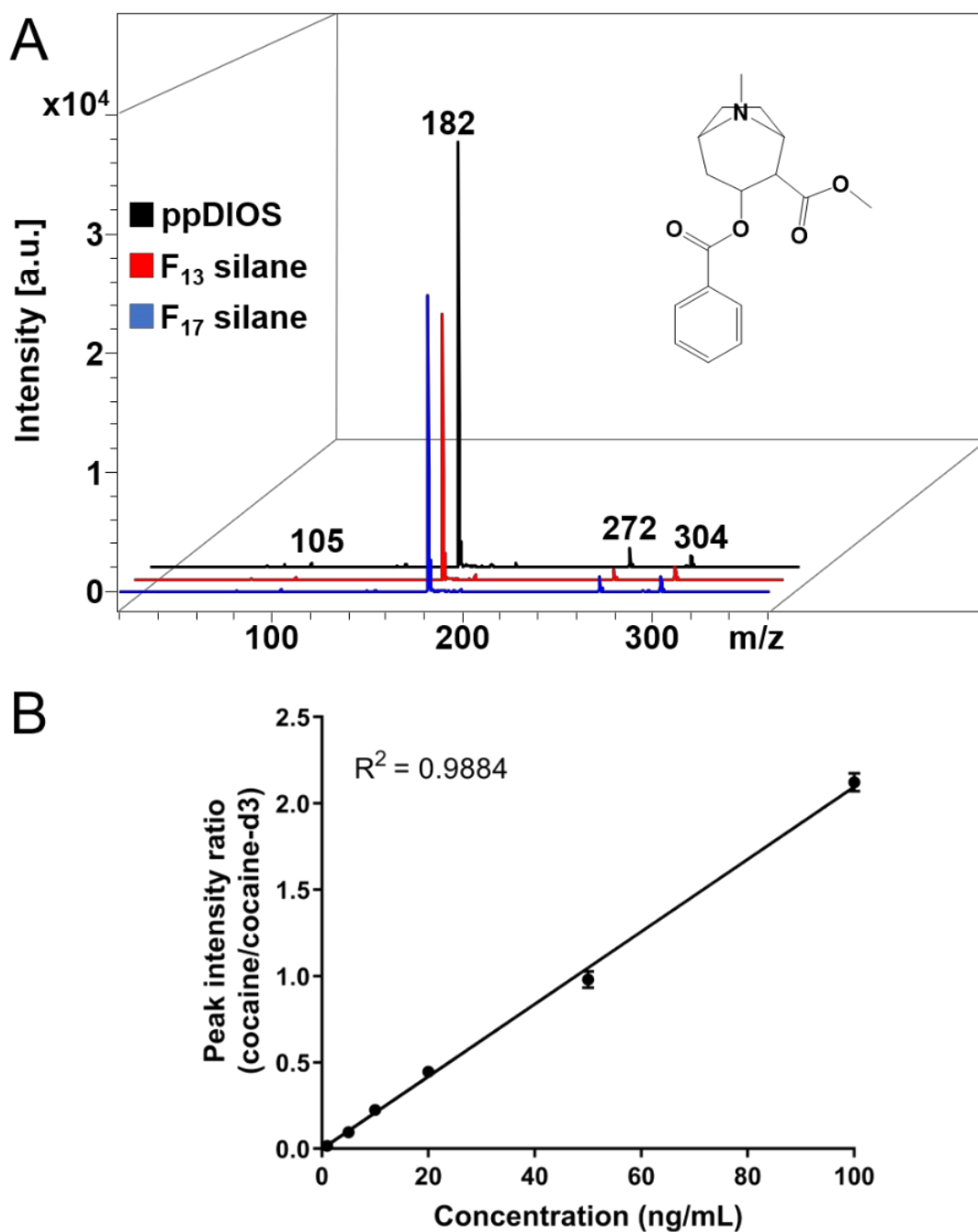


Figure S10. (A) Representative mass spectrum for cocaine (100 ng/mL, in water) at an ion of m/z 304, analysed using DIOS-MS on a ppDIOS surface. Fragment peaks are observed at m/z 105, m/z 182 and m/z 272. (B) Linear regression curve for cocaine in water for concentrations ranging from 1 to 100 ng/mL. Error bars correspond to the standard deviation ($n=3$).

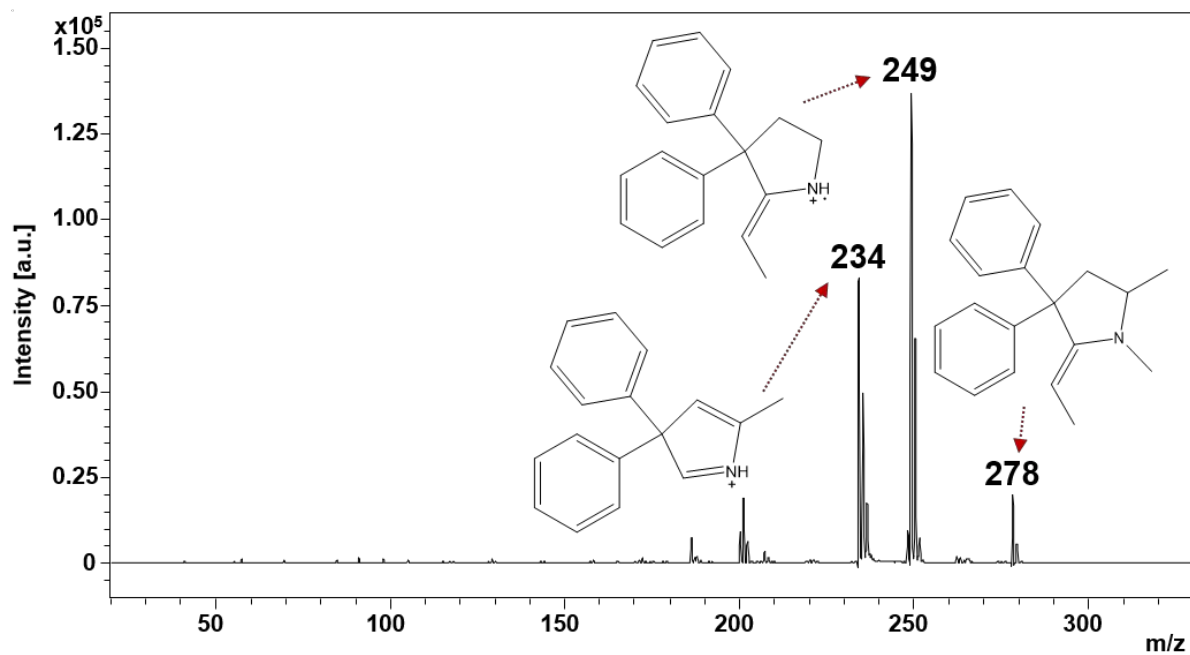


Figure S11. MS/MS mass spectrum for EDDP, a major urinary metabolite of methadone, at an ion of m/z 278, analysed using an F_{13} -silanised DIOS surface. Fragment peaks are observed at m/z 234 and m/z 249.

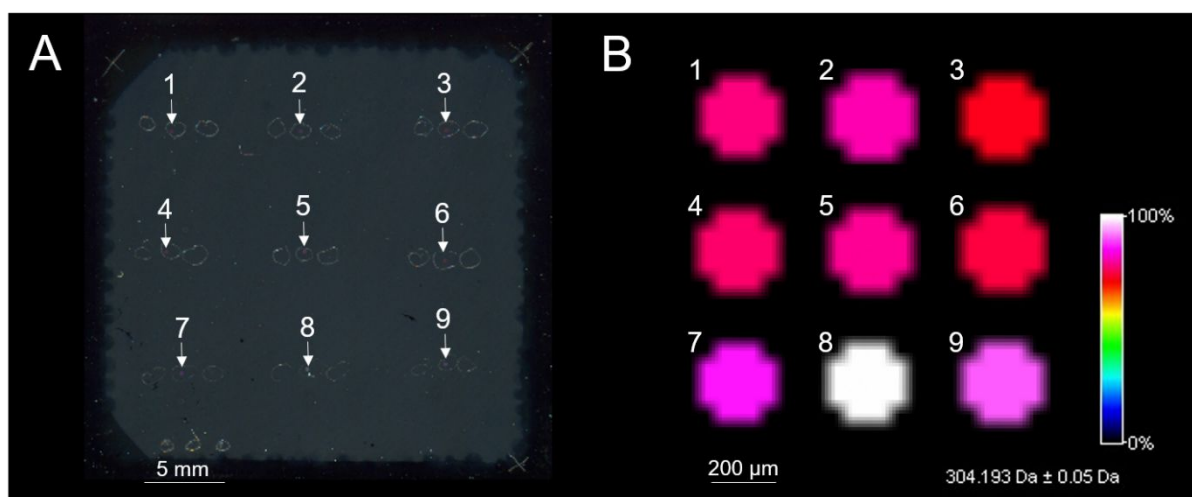


Figure S12: ppDIOS imaging of cocaine (100 ng/mL in chloroform) showing: A) a spot array where analysis was performed from nine different locations throughout the ppDIOS surface, and B) zoomed-in view of each of the imaged spots. The parent peak of cocaine was detected at m/z 304. An arbitrary colour scale detailing the relative intensity of each peak is displayed to the right.

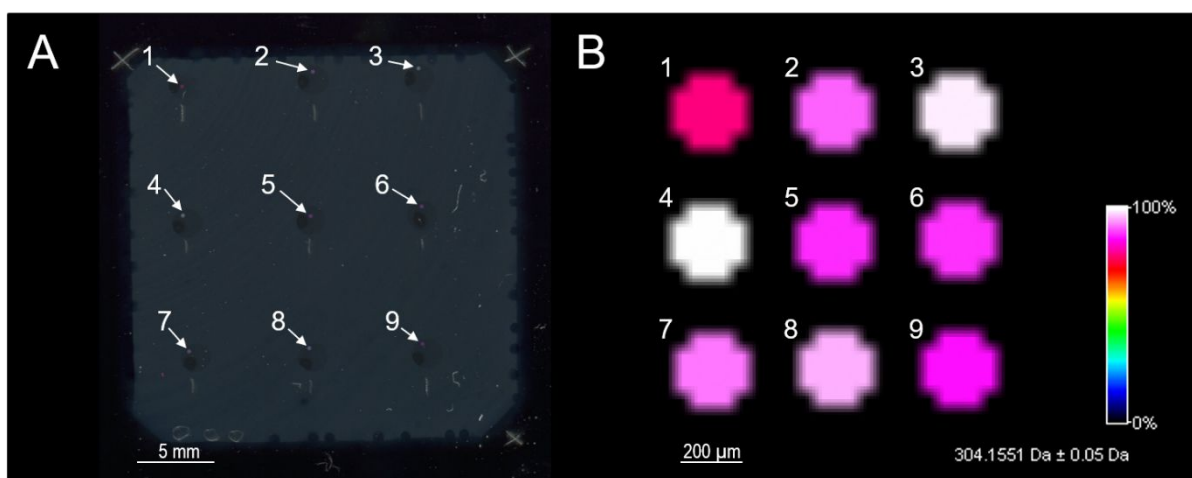


Figure S13: DIOS imaging of cocaine (100 ng/mL in chloroform) showing: A) a spot array where analysis was performed from nine different locations throughout the DIOS surface, and B) zoomed-in view of each of the imaged spots. The parent peak of cocaine was detected at m/z 304. An arbitrary colour scale detailing the relative intensity of each peak is displayed to the right. Reprinted with permission from (1). Copyright (2020) American Chemical Society.

References

1. Minhas, R. S.; Rudd, D. A.; Al Hmoud, H. Z.; Guinan, T. M.; Kirkbride, K. P.; Voelcker, N. H., Rapid Detection of Anabolic and Narcotic Doping Agents in Saliva and Urine By Means of Nanostructured Silicon SALDI Mass Spectrometry. *ACS Applied Materials & Interfaces* **2020**, 12 (28), 31195-31204.